Sixth International Symposium on Marine Propulsors
smp'19, Rome, Italy, May 2019

A Practical Calculation Method of Pressure Fluctuation Induced by Cavitating Propeller Using a Simple Surface Panel Method "SQCM"

Takashi Kanemaru[1], Daijiro Arakawa[2], Yuki Sawada[2], Koichiro Shiraishi[2], Jun Ando[1]

[1]Faculty of Engineering, Kyushu University, Fukuoka, Japan
[2]National Maritime Research Institute, Tokyo, Japan

ABSTRACT

This paper presents a practical calculation method for pressure fluctuation induced by cavitating propeller. The method is based on a simple surface panel method "SQCM" and treats the three types of cavitation, sheet cavitation, tip super cavitation and tip vortex cavitation.

The calculation method based on a potential flow theory is generally expected to be light calculation load for the initial stage of propeller design. However, it is difficult to satisfy the need because it must be able to calculate not only cavity area but also cavity volume in order to predict the pressure fluctuation theoretically.

The present method in this paper improves the authors' previous method (Kanemaru et al 2015) for the practicability with maintaining the accuracy as much as possible. The main feature in this method is that the cavitation calculation is conducted about key blade only, in other words, about one blade propeller. The interaction between blades is considered using the data of inflow velocity components from other blades to the key blade, which is calculated without cavitation in advance. The calculated cavitation pattern, cavity volume and pressure fluctuation are shown comparing with the experimental data.

Keywords

SQCM (Source and QCM), Cavity Volume, Pressure Fluctuation, Amplitude of Blade Frequency

1 INTRODUCTION

Unsteady cavitation due to ship wake produces the considerable pressure fluctuation on ship stern, which causes the hull vibration and structural damage. Therefore, it is very important to predict the pressure fluctuation induced by cavitating propeller in the propeller design stage.

We presented the calculation methods of propeller cavitation at smp'09 (Kanemaru et al 2009) and pressure fluctuation induced by the cavitation at smp'11 (Kanemaru et al 2011). These methods are based on a simple surface panel method "SQCM" which was developed by Kyushu University (Ando et al 1998). The feature of the cavitation calculation is that the cross flow component around blade tip is taken into consideration in free streamline theory which solves the sheet cavity shape theoretically. Furthermore, we added tip cavitation model to the calculation method of sheet cavitation (Kanemaru et al 2015). The tip cavitation model consists of tip vortex cavitation model and tip super cavitation model which treats undeveloped local super cavitation near the tip.

The developed method can calculate the time variation of the cavity volume which is important for the prediction of pressure fluctuation in practical computation time. It can be said that the method has both the practicability and the accuracy. However, there are some cases that the very quick estimation is required and our method is not so light calculation load.

The reason of the calculation load is that the method is too precise according to theories for the accurate simulation. Nonlinear analysis of cavitating flow needs the much times of iterative calculations for the converged cavity shape and cavity length. But nonlinear theory is indispensable for the prediction of pressure fluctuation even if it is heavy.

In this study, we modify the previous method (Kanemaru et al 2017) for more practical method. The calculation method of cavitation is divided into two steps. The first step is calculation of inflow velocity vector from other blades to key blade without cavitation. The second step is the calculation of cavity shape on the key blade. In this step, the cavitation calculation is conducted about key blade only and the interaction between blades is considered using the data of inflow velocity vector calculated by the previous step. The present method keeps the nonlinear cavitating analysis but the matrix size becomes much smaller.

[*] Leave blank the last 2.0 cm on the first page to place some additional informational about this paper in a footnote on the first page if necessary.

The calculated results of cavity volume, cavitation patterns, fluctuating pressure are shown about two types of propellers and these results are compared with experimental data and the previous method.

2 CALCULATION

SQCM (Source and QCM) uses source distributions (Hess & Smith 1964) on the propeller blade surface and discrete vortex distributions arranged on the mean camber surface according to QCM (Quasi-Continuous vortex lattice Method) (Lan 1974), which is well known as one of lifting surface methods. The formulation of SQCM is described in the papers (Ando et al. 1998, Kanemaru et al 2009). We applied SQCM to the calculation method of unsteady propeller cavitation and pressure fluctuation induced by the cavitation (Kanemaru et al 2011). Also, the paper (Kanemaru et al 2017) describes the calculation method for tip vortex cavitation and tip super cavitation using bubble tracing method.

This paper presents the method of cavitation calculation for only key blade and the simplified method for pressure fluctuation induced by the cavitation.

2.1 Modeling of one blade propeller

Figure 1 shows the series of calculations for the cavitation and the pressure fluctuation by the previous method.

First of all, the advance velocity satisfying the target thrust coefficient K_T which is one of the calculation conditions is calculated (Step 1a). This advanced velocity can be calculated by interpolation of three points interposing the target advanced velocity. This calculation is conducted without cavitation assuming that the propeller performance does not change regardless of cavitating condition.

Next, the unsteady cavitation calculation is conducted setting the advanced velocity by Step 1a and giving the data of ship wake (Step 2a). In this step, the cavity shapes at each time step are calculated and the data of cavity shapes are put out as the data file. Here, the cavitation calculation is conducted about only key blade. Other blades are calculated without cavitation and QCM is applied to these blades in order to save the computation time.

The calculation of pressure fluctuation (Step 3a) is conducted using the cavity shape data by Step 2a. Here the calculated cavity shapes are given at all blades. In the case of flat plate model, mirror image is applied.

This previous method takes about one day to conduct these calculations though it depends on the calculation condition. It is by no means light calculation load for the initial stage of propeller design though it is much faster comparing with CFD.

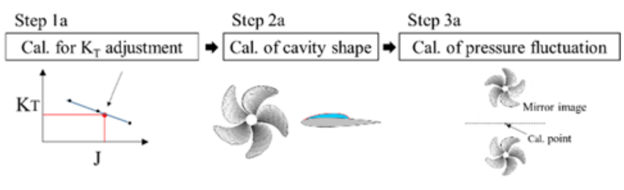

Figure 1: Series of calculation (Previous method)

There are two main reasons of the calculation load in the previous method. One is the nonlinear analysis of cavitating flow which needs much iterative calculations in order to obtain the converged cavity shape and cavity length. However, this process is inevitable because the time variation of the cavity volume must be calculated accurately for the prediction of pressure fluctuation. The other is that the control points on the source panels change at each calculation for solving the cavity shape and cavity length. Therefore, the singularity distributions at each calculation must be solved without inverse matrix operation method though it is used in the case without cavitation. In order to use the method, the calculation must be conducted in propeller fixed coordinate system in rotating ship wake relatively and the panel arrangement must not change. This operation problem is very difficult to be solved in cavitation calculation.

In this study, we try to make the matrix size small as the fundamental solution of the problem.

Figure 2 shows the series of calculations by the present method. The first step (Step 1b) for K_T adjustment is same to Step 1a in **Figure 1**. In the present method, we introduce Step 2b before cavitation calculation. Step 2b calculates the inflow velocity vectors from other blades to key blade without cavitation and with constant control points. Step 2b can be calculated using propeller fixed coordinate system and the computation time is small.

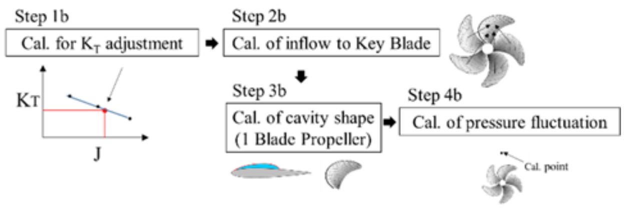

Figure 2: Series of calculation (Present method)

Next, the cavitation calculation is conducted (Step 3b). Here, the calculation treats only key blade, namely, one blade propeller. The interaction between blades which is important for propeller calculation is considered using the data of inflow velocity vector from the other blades, which is calculated in Step 2b. In this treatment, cavity on the other blades are out of consideration. Step 3b is very fast comparing with Step 2a because of the small matrix size. As the results, the present method becomes much faster than the previous method.

The boundary condition on the key blade surface is given as follow:

$$\vec{V} \cdot \vec{n} = 0 \tag{1}$$

Here, $\vec{V}$ is the velocity vector on the key blade surface and $\vec{n}$ is the unit normal vector on the control point. $\vec{V}$ in the previous method is expressed as:

$$\vec{V} = [\,\vec{V}_I\,] + \vec{V}_{\gamma K} + \vec{V}_{mK} + \vec{V}_{\gamma o} + \vec{V}_{mo} \tag{2}$$

Here, $\vec{V}_I$ is the inflow velocity vector by the working condition including ship wake, $\vec{V}_{\gamma K}$ and $\vec{V}_{mK}$ are induced velocity vectors by vorticities distribution and source distribution of the key blade itself. $\vec{V}_{\gamma o}$ and $\vec{V}_{mo}$ are induced velocity vectors by those of other blades and [ ] shows the known value substituted as input data. The present method can be expressed as follows:

$$\vec{V} = \left[\, \vec{V}_I \,\right] + \vec{V}_{\gamma K} + \vec{V}_{mK} + \left[\vec{V}_{\gamma o} + \vec{V}_{mo}\right] \qquad (3)$$

Namely, $\vec{V}_{\gamma o}$ and $\vec{V}_{mo}$ are not calculated values but input values and the matrix size becomes 1/(the number of blade). Actually, the matrix size is about a half of that by the previous method in the case of four blades propeller because the previous method already applies the coarse panel to other blades for saving computation time.

2.2 Calculation method of pressure fluctuation

In the previous method, the cavity shape of key blade calculated in Step 2a are applied to all blades considering the each phase angle and the calculation of pressure fluctuation is conducted. Also, the mirror image is used in order to express the flat plate as shown in **Figure 1** (Step 3a). In this case, it is impossible to use inverse matrix operation method because the positional relation of control points between both propellers is not constant.

In this study, the equation of pressure fluctuation by the second time derivative of the spherical cavity volume (Hoshino 1979) is applied as shown in Equation (4).

$$\Delta p(t) = \alpha \frac{\rho}{4\pi\ell} \frac{d^2 V_C}{dt^2} \qquad (4)$$

Here, $\Delta p(t)$ is the half amplitude of fluctuating pressure, ρ is the density of the fluid, ℓ is the distance between the estimation point and the center of the cavity, V_C is the cavity volume and t is the time. Actually, the fluctuating pressure is smaller than that by Equation (4). α is the coefficient to attenuate the pressure fluctuation. The coefficient of the pressure fluctuation ΔK_p is defined as follow:

$$\Delta K_p = \frac{\Delta p(t)}{\rho n^2 D_p^2} \qquad (5)$$

Here, n and D_p is the revolutions per second and the propeller diameter. ΔK_p can be expressed using Fourier series as follow:

$$\Delta K_p = -\sum_{i=1} K_{piN} \cdot cos(iN(\theta - \varphi_{iN})) \qquad (6)$$

Here, K_{piN} and φ_{iN} are the amplitude and phase of i-th order frequency component. N is the number of blades.

3 Validation

In this study, we take two types of propellers, a coasting vessel propeller (M.P.700 (Kawakita et al 2017)) and Seiun-Maru-I highly skewed propeller (HSP-II) for the validation of the present method. **Table 1** shows the principal particulars and **Figure 3** and **4** show the model propellers for the experiment and the panel arrangements for the cavitation calculation. The experiment was conducted in Large Cavitation Tunnel in National Maritime Research Institute (Arakawa et al 2018). **Figure 5** shows the test section and the location of pressure transducer of the flat plate.

Table 1: Principal particulars of propellers

	M.P.No.700	Seiun-Maru-I HSP-II
Diameter D_p [m]	0.240	0.250
Pitch ratio at 0.7R	0.6059	0.9940
Expanded area ratio	0.4791	0.7000
Boss ratio	0.1750	0.1972
Number of blade Z	4	5
Skew angle [deg]	25.0	45.0
Rake angle [deg]	4.13	-3.03
Blade section	NACA	Modified SRI-B
Direction of rotation	Right	Right

M.P.No.700 Seiun-Maru-I HSP-II

Figure 3: Model propellers

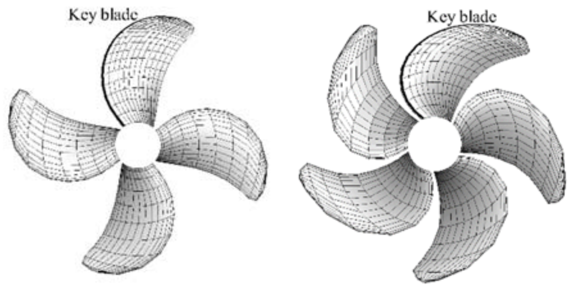

M.P.No.700 Seiun-Maru-I HSP-II

Figure 4: Panel arrangements for cavitation model

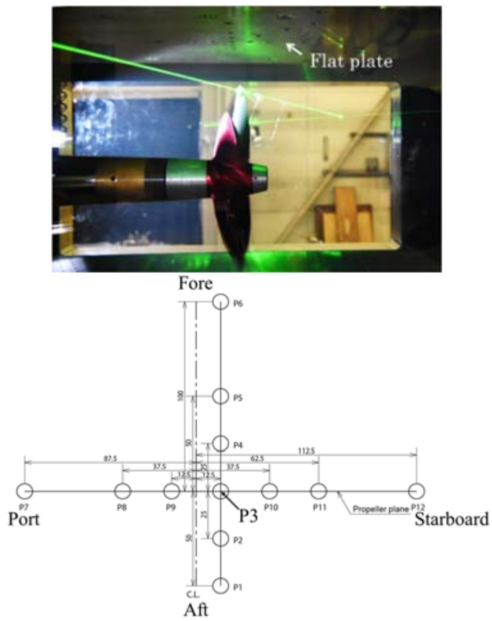

Figure 5: Location of pressure transducer on flat plate

Figure 6 shows the wake distributions on the propeller plane by wire mesh screen regarding M.P.700 and Seiun-Maru-I HSP-II respectively.

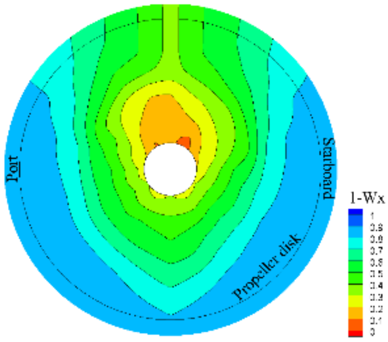

M.P.No.700

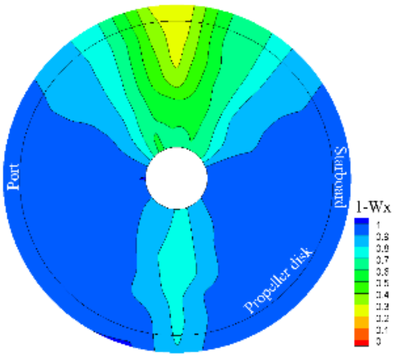

Seiun-Maru-I HSP-II

Figure 6: Axial wake distributions

3.1 Coasting vessel propeller M.P.No.700

Figure 7 compares the calculated cavitation patterns with the experimental data at each phase angle. The calculated results can express the experimental phenomenon of the cavity development and the collapse.

Figure 8 and **9** show the calculated cavity area and cavity volume comparing with those by the previous method. The difference between these calculated results is very small regarding both cavity area and cavity volume. It is confirmed that the interaction effect between blades can be expressed by the input data of inflow velocity vector from other blades to key blade and the one blade cavitation calculation has enough accuracy.

Figure 10 and **11** show the longitudinal and the transverse amplitude distribution of pressure distribution on the flat plate in the case without cavitation. In this case, the fluctuating pressure has almost only the 1st order frequency component and the calculated results agree well with the experimental data.

Figure 12 and **13** show the amplitude distribution of pressure fluctuation in the case with cavitation. The calculated results are similar to the experimental data regarding the 1st order frequency component. The calculated peak point does not correspond to that by the experimental data because there is a phase angle difference between calculation and experiment.

Figure 14 and **15** show the amplitude of pressure fluctuation at P3 (**Figure 5**). In the case without cavitation, the calculated results agree well with the experimental data. In the cavitating condition, the 2nd order frequency component is difficult to be simulated by the calculation.

On the other hand, the difference between the present method and the previous method is very small. It can be said that the fast calculation by the present method keeps the equivalent accuracy to the previous method.

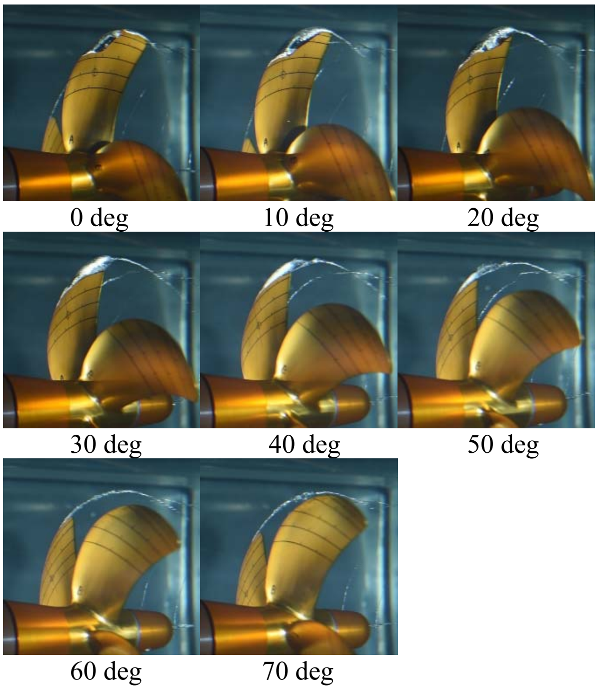

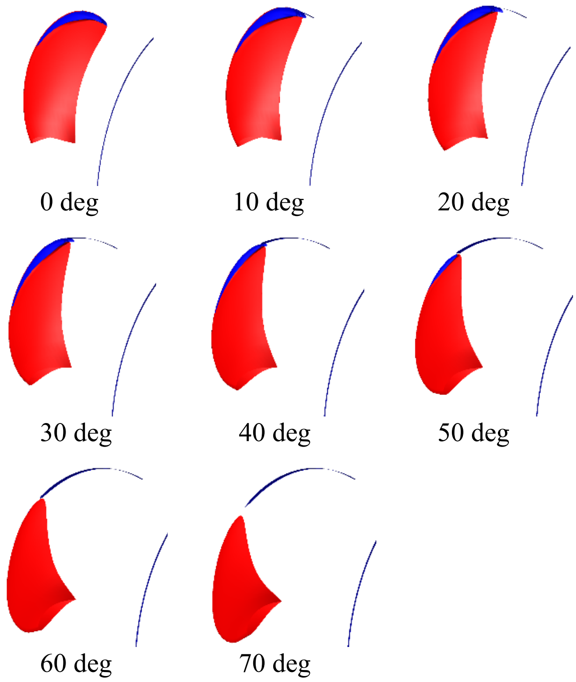

Figure 7: Cavitation patterns of M.P.No.700 (K_T=0.124, σ_{nc}=1.37 , upper:EXP., lower:CAL.)

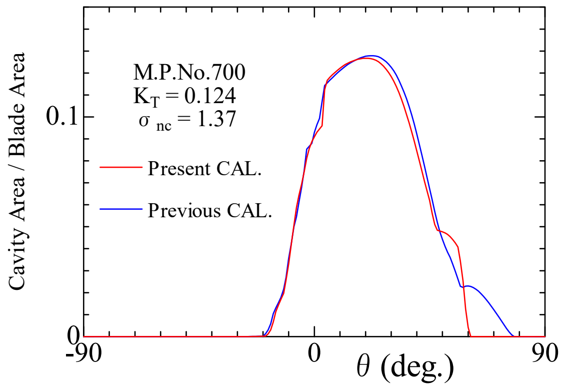

Figure 8: Calculated cavity area of M.P.No.700

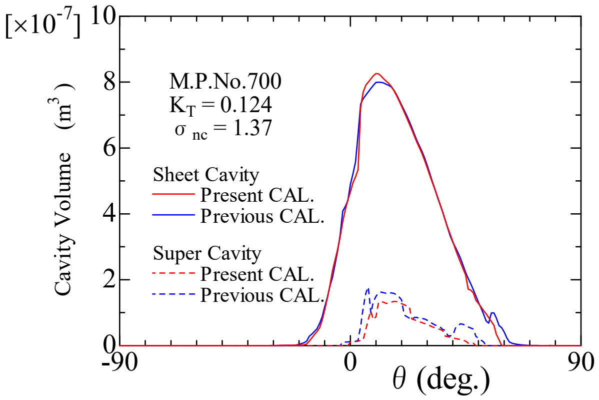

Figure 9: Calculated cavity volume of M.P.No.700

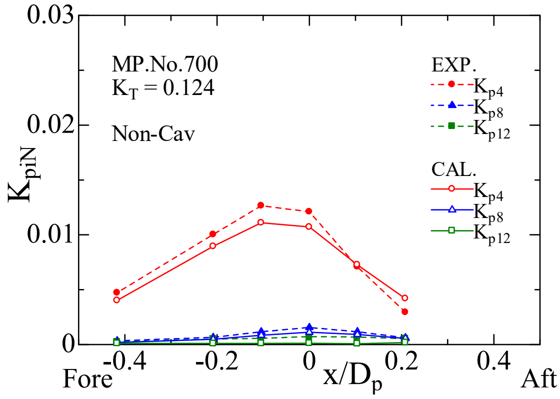

Figure 10: Amplitude distribution of pressure fluctuation of M.P.No.700 (Non-Cav, Longitudinal direction)

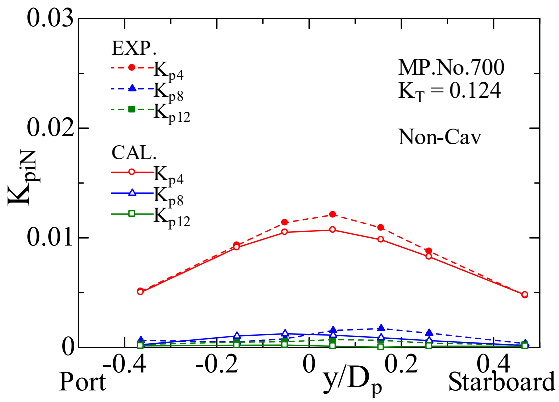

Figure 11: Amplitude distribution of pressure fluctuation of M.P.No.700 (Non-Cav, Transverse direction)

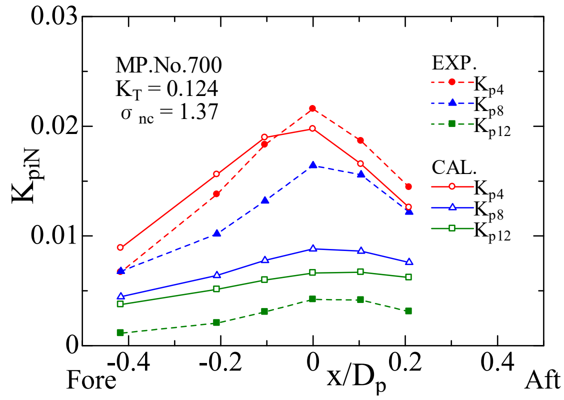

Figure 12: Amplitude distribution of pressure fluctuation of M.P.No.700 (w/Cav, Longitudinal direction)

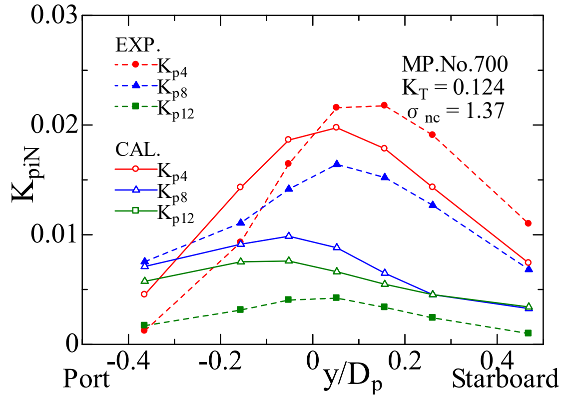

Figure 13: Amplitude distribution of pressure fluctuation of M.P.No.700 (w/Cav, Transverse direction)

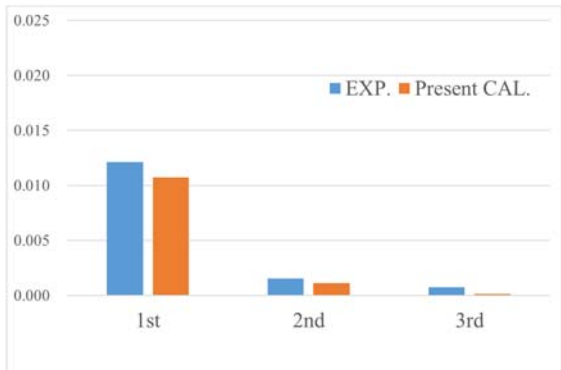

Figure 14: Amplitude of pressure fluctuation K_{piN} at P3 (M.P.No.700, Non-Cav, K_T=0.124, σ_{nc}=1.37)

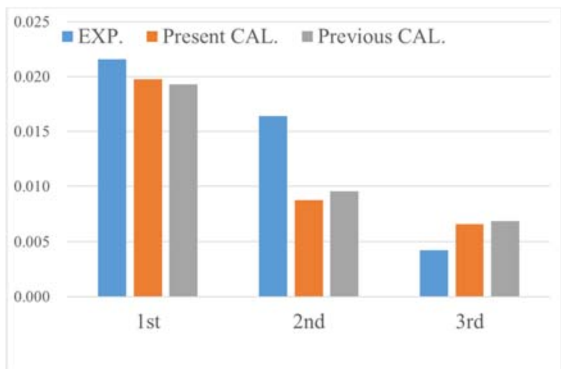

Figure 15: Amplitude of pressure fluctuation K_{piN} at P3 (M.P.No.700, w/Cav, K_T=0.124, σ_{nc}=1.37)

3.2 Seiun-Maru-I HSP-II

Figure 16 shows the experimental and calculated cavitation patterns at each phase angle. If the difference of phase angle by 10 degrees between the experiment and the calculation is considered, it can be said that the calculated cavitation patterns express those of experiment.

Figure 17 and **18** show the calculated cavity area and cavity volume. These variations to the phase angle is a little complicated, especially in the shrinking phase.

Figure 19 and **20** show the transverse amplitude distribution of pressure fluctuation in the case without and with cavitation. The calculated result with peak position modification agrees with the experimental data regarding the 1st and the 2nd order frequency components in non-cavitation. However, the calculated results with cavitation are far from the experimental data in the port side.

Figure 21 and **22** show the amplitude of pressure fluctuation at P3 (**Figure 5**). If the point P3 is focused on, the calculated amplitude of pressure fluctuation can express the experimental data regarding not only non-cavitating condition but also cavitating condition including the 2nd order frequency component.

Figure 23 shows the fluctuating pressure in one revolution at P3 in the case with cavitation. If the difference of phase angle by 15 degrees between the experiment and the calculation is considered, the wave pattern of fluctuating pressure by the calculation is similar to that by the experiment.

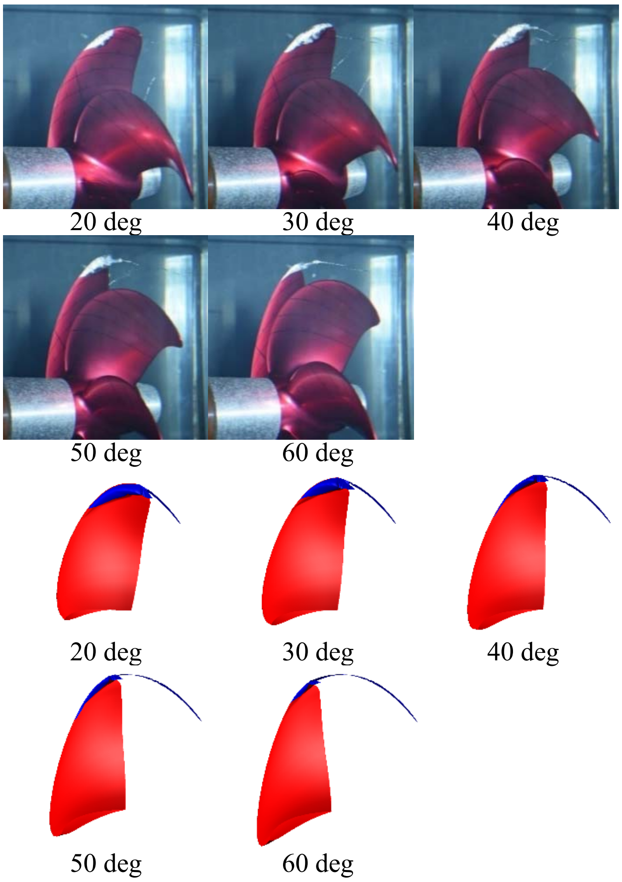

Figure 16: Cavitation patterns of Seiun-Maru-I HSP-II (K_T=0.201, σ_{nc}=2.99, upper:EXP., lower:CAL.)

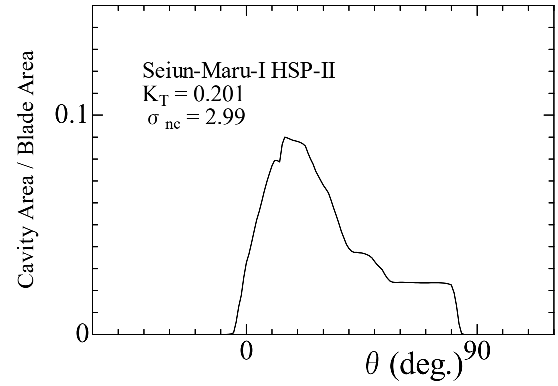

Figure 17: Calculated cavity area of Seiun-Maru-I HSP-II

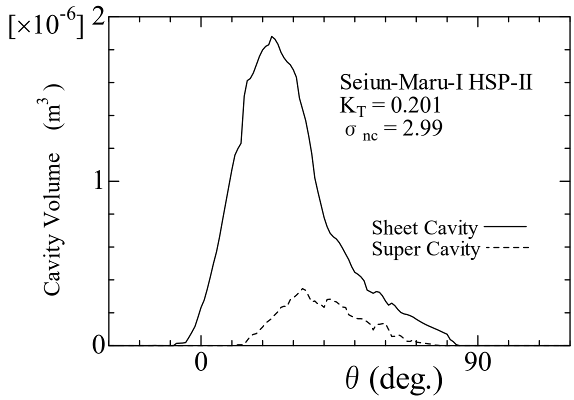

Figure 18: Calculated cavity volume of Seiun-Maru-I HSP-II

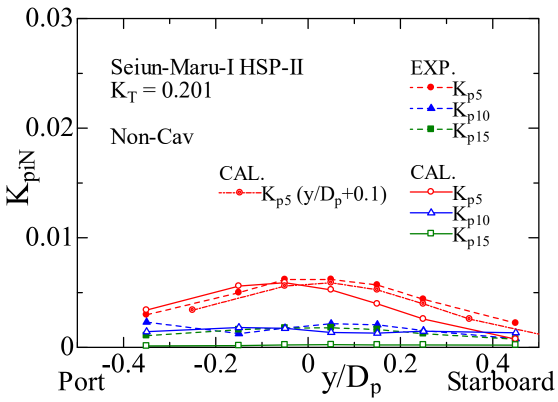

Figure 19: Amplitude distribution of pressure fluctuation of Seiun-Maru-I HSP-II (Non-Cav, Transverse direction)

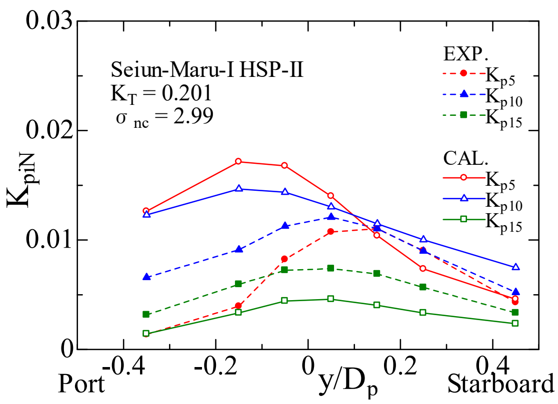

Figure 20: Amplitude distribution of pressure fluctuation of Seiun-Maru-I HSP-II (w/Cav, Transverse direction)

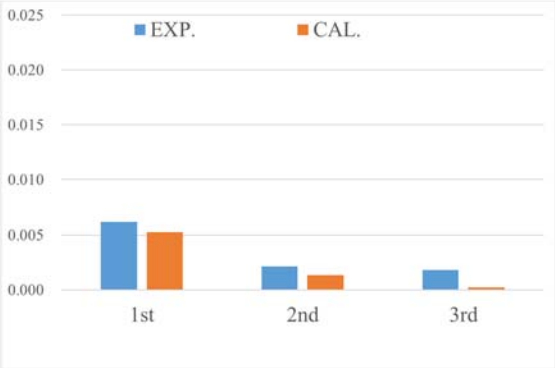

Figure 21: Amplitude of pressure fluctuation K_{piN} at P3 (Seiun-Maru-I HSP-II, Non-Cav, K_T=0.201, σ_{nc}=2.99)

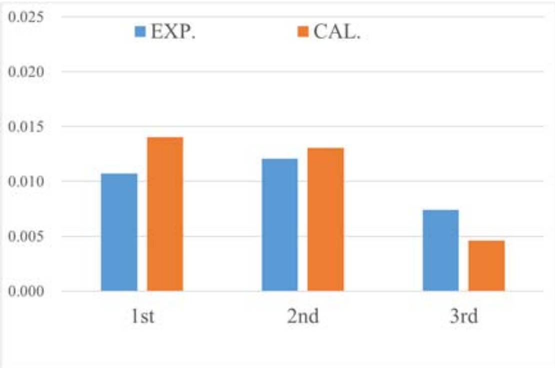

Figure 22: Amplitude of pressure fluctuation K_{piN} at P3 (Seiun-Maru-I HSP-II, w/Cav, K_T=0.201, σ_{nc}=2.99)

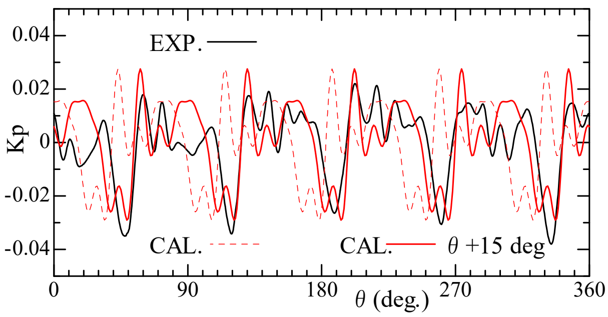

Figure 23: Fluctuating pressure in one revolution at P3 (Seiun-Maru-I HSP-II, w/Cav, K_T=0.201, σ_{nc}=2.99)

4 CONCLUSIONS AND FUTURE WORK

In this paper, we present the practical calculation method for the pressure fluctuation induced by cavitating propeller by improving the previous method which conducts the cavitation calculation exactly. The present method calculates the cavitating propeller about one blade propeller and the interaction effect between blades are considered using the data of inflow velocity vector from other blades to key blade, which is calculated in advance. Furthermore, the second time derivative of the cavity volume is applied for the calculation method of pressure fluctuation.

The present method keeps the accuracy which is comparable to the previous method regarding cavity area, cavity volume and amplitude of the pressure fluctuation. Also, the calculated cavitation patterns are agreed with those of experiment by considering the phase angle difference.

In the case without caviation, the calculated pressure fluctuation agrees well with the experimental data.

On the other hand, the amplitude distribution of pressure fluctuation is difficult to be simulated. However, the calculated amplitudes including higher order frequency components at right above point from the propeller agree with the experimental data regarding Seiun-Maru-I HSP-II. In addition, it can be seen that the calculated fluctuating pressure is similar to that by the experiment.

The computation time is about one-fifth comparing with that of the previous method. It can be said that the present method is innovative from the point of view of practicability.

The quantitative and qualitative difference between calculation and experiment depends on the propeller. The development of more accurate prediction method for pressure fluctuation is our future work.

REFERENCES

Ando, J., Maita, S. & Nakatake, K. (1998). 'A New Surface Panel Method to Predict Steady and Unsteady Characteristics of Marine Propeller'. Proceedings of 22st Synposium on Naval Hydrodynamics, Washington D.C., pp. 142-154.

Arakawa, D., Shiraishi, K., Sawada, Y. & Kawakita, C. (2018). 'Study on Experiment on Pressure Fluctuation Induced by Propeller and Cavitation'. Conference Proceedings The Japan Society of Naval Architects and Ocean Engineers, Vol.26, pp. 563-568.

Hess, J.L. & Smith, A.M.O. (1964). 'Calculation of Nonlifting Potential Flow about Arbitrary Three Dimensional Bodies'. Journal of Ship Research, Vol.8, No.2, pp. 22-44.

Hoshino, T. (1979). 'Pressure Fluctuation Induced by a Spherical Bubble Moving with Varying Radius'. Transactions of the West-Japan Society of Naval Architects, Vol.58, pp. 221-234.

Kanemaru, T. & Ando, J. (2009). 'A Numerical Analysis of Steady and Unsteady Sheet Cavitation on a Marine Propeller Using a Simple Surface Panel Method "SQCM" '. Proceedings of 1st International Synposium on Marine Propulsor, Trondheim, pp. 372-379.

Kanemaru, T. & Ando, J. (2011). 'Numerical Analysis of Pressure Fluctuation on Ship Stern Induced by Cavitating Propeller Using a Simple Surface Panel Method "SQCM" '. Proceedings of 2nd International Synposium on Marine Propulsor, Hamburg, pp. 116-123.

Kanemaru, T. & Ando, J. (2015). 'Numerical Analysis of Tip Vortex Cavitation on Marine Propeller Using a Simple Surface Panel Method "SQCM" '. Proceedings of 4th International Synposium on Marine Propulsor, Austin, pp. 505-512.

Kawakita, C., Shiraishi, K., Fujisawa, J., Sawada, Y., & Arakawa, D. (2017). 'Development of Fixed Pitch Propellers for Coasting Vessels'. Conference Proceedings The Japan Society of Naval Architects and Ocean Engineers, Vol.24, pp. 169-174.

Lan, C.E. (1974). 'A Quasi-Vortex-Lattice Method in Thin Wing Theory'. Journal of Aircraft, Vol.11, No.9, pp. 518-527.